Fe2+−Mg order-disorder in orthopyroxene: Equilibrium fractionation between the octahedral sites and thermodynamic analysis

Article *in* Contributions to Mineralogy and Petrology · September 1999

DOI: 10.1007/s004100050540

CITATIONS
59

READS
74

3 authors, including:

M. Stimpfl
The University of Arizona
40 PUBLICATIONS **533** CITATIONS

SEE PROFILE

Jibamitra Ganguly
The University of Arizona
199 PUBLICATIONS **6,738** CITATIONS

SEE PROFILE

Contrib Mineral Petrol (1999) 136: 297–309

M. Stimpfl · J. Ganguly · G. Molin

Fe^{2+}-Mg order-disorder in orthopyroxene: equilibrium fractionation between the octahedral sites and thermodynamic analysis

Received: 25 August 1998 / Accepted: 10 March 1999

Abstract The equilibrium intracrystalline distribution coefficient, k_D^*, of Fe^* (i.e. Fe^{2+} + Mn) and Mg between the M1 and M2 sites of three natural nearly binary Fe^{2+}-Mg orthopyroxene crystals (Fs_{14}, Fs_{15} and Fs_{49}) were determined by annealing experiments at several temperatures between 550 and 1000 °C and single crystal X-ray structure refinements. In addition, the X-ray data of an orthopyroxene crystal (Fs_{23}), which were collected earlier by Molin et al. (1991) between 700 and 1000 °C, were re-refined. The data were processed through two different refinement programs (SHELXL-93 and RFINE90) using both unit and individual weights and also both ionic and atomic scattering factors. The calculated site occupancies were found to agree within their estimated standard errors. However, the use of ionic scattering factors led to significantly better goodness of fit and agreement index, and smaller standard deviations of the site occupancies than those obtained from the use of atomic scattering factors. Furthermore, the weighted refinements yielded significantly smaller standard deviations of the site occupancies than the unweighted refinements even when the same set of reflections was used in the two procedures. The site occupancy data from this study were combined with selected published data to develop expressions of k_D^* as a function of temperature and composition. Calculation of the excess configurational entropy, ΔS^{XS}, suggests that orthopyroxene should be treated as a *two parameter* symmetric solution instead of as a "simple mixture". The calculated ΔS^{XS} values and the excess Gibbs free energy of mixing suggested by available cation exchange data lead to a slightly negative enthalpy of mixing in the orthopyroxene solid solution.

M. Stimpfl (✉) · J. Ganguly
Department of Geosciences, University of Arizona, Tucson, AZ 85721, USA

G. Molin
Dipartimento di Petrografia e Mineralogia, Universita' di Padova, I-35137 Padova, Italy

Introduction

In orthopyroxenes, Fe^{2+} and Mg fractionate between two nonequivalent octahedral sites, M1 and M2, with Fe^{2+} preferring the larger of the two sites (Ghose 1965). The principal geological interest in this problem stems from its potential application to the determination of cooling rates of terrestrial and extraterrestrial rocks (Ganguly 1982; Anovitz et al. 1988; Skogby 1992; Ganguly et al. 1994; Molin et al. 1994a,b; Artioli and Davoli 1995; Ganguly and Domeneghetti 1996; Zema et al. 1997; Ganguly et al. 1997; Kroll et al. 1997). However, the determination of cooling rate from the observed Fe-Mg ordering state requires accurate data on the equilibrium site fractionation and the kinetics of the fractionation process of these cations. It is also very sensitive to small errors in the site occupancy data, especially for low Fe concentration (Ganguly et al. 1989; Kroll et al. 1997). We report in this paper the results of experimental study on the equilibrium site fractionation in three natural orthopyroxene crystals (Fs_{14}, Fs_{15} and Fs_{49}) as a function of temperature, as determined by annealing experiments and single crystal X-ray structure refinements. In addition, we have re-determined the chemical composition and re-refined the X-ray data of Molin et al. (1991) of an orthopyroxene crystal (Fs_{23}) from the Johnstown meteorite, which was annealed at several temperatures between 700 and 1000 °C, using different strategies. The need for the type of experimental data presented in this work is highlighted by the recent critical analysis of Kroll et al. (1997), who concluded that "the large range of reported results is disconcerting", and emphasized the need for "new, accurate and consistent site occupancies, the more so if thermodynamic properties of orthopyroxene solid solution are to be derived from the coefficients of statistically fitted thermodynamic models to the data". Finally we also discuss the implications of the site partitioning data for the thermodynamic mixing properties of the orthopyroxene solid solution.

The closure temperature (T_C) of cation ordering, obtained by comparing its quenched ordering state with a calibration of equilibrium ordering state versus temperature, plays a critical role in the retrieval of its cooling rate (Ganguly 1982). However, since different structure refinement programs use different strategies, Ganguly et al. (1994) recommended that the site occupancy determination of an unknown sample should be carried out in the same way as that used in the calibration of equilibrium site occupancy as a function of temperature. It was hoped that in this approach, any inherent error in the site occupancy determination arising from a particular structure refinement strategy would be self compensating between the unknown and the calibrated samples. Kirfel (1996) carried out an interlaboratory comparison of cation distribution studies using the same X-ray data sets for olivine and orthopyroxene crystals, and found considerable disagreement among the results. He, thus, reinforced the recommendation of Ganguly et al. (1994). As an alternative, he suggested determination of the site occupancies using "multiple refinement approach". In this work, we also compare results of site occupancy determination obtained by subjecting the same X-ray data for a crystal to different refinement strategies in order to isolate the differences arising from those in the refinement schemes, and to recommend a good working procedure.

Experimental procedure

We separated several crystals of orthopyroxene from two samples of stony-iron (type IVA) meteorites, Steinbach and São João Nepomuceno (Haack et al. 1996), and from a terrestrial granulite facies sample from the Central Gneiss Complex of British Columbia, Canada (Hollister 1982, sample number TPK 30F). From these crystals, we selected two crystals from São João Nepomuceno and one from each of the rest that were best suited for X-ray structure refinements, and determined their initial ordering states without bulk compositional constraints. The selected crystals from São João Nepomuceno (Fs_{14}), Steinbach (Fs_{15}) and granulite (Fs_{49}) were labeled SJN(23 and 25), ST77 and HO28, respectively.

Each crystal was disordered successively at several temperatures up to 1000 °C for sufficiently long duration to achieve a steady state as determined by time series study. After completion of the disordering experiments, the crystals were successively ordered at the same set of temperatures. Thus, the equilibrium ordering state at each temperature was "reversed", that is established by approaching it from the states which were initially more ordered and more disordered than the equilibrium state. The annealing experiments were carried out by sealing each crystal, along with a physically separated mixture of wüstite and iron, in a silica tube in the presence of a flowing Ar gas. The assembly was then suspended at the "hot spot", which was calibrated to be ~5 cm long, in a vertical tube furnace, and drop-quenched in water. The furnace was always preheated to the desired temperatures before insertion of the samples. Temperature was monitored by a chromel-alumel or a Pt-Pt10%Rh thermocouple with its junction placed at essentially the same horizontal section of the furnace as that containing the sample. The separation between the thermocouple junction and the sample was ≤0.5 cm.

After each annealing experiment, the crystal was mounted on a single crystal diffractometer for X-ray data collection, and then subjected to the next experimental cycle. Except for SJN, only one crystal was used for the entire calibration of distribution coefficient versus temperature at a fixed bulk composition. After completion of the annealing experiments and X-ray data collections, each crystal was analyzed in an electron microprobe, and treated according to a projection scheme, as discussed later, to determine its statistically most probable bulk composition.

X-ray structure refinements and site occupancy determinations

Single crystal X-ray intensity data were obtained using either a Siemens AED II or a NONIUS CAD-4 four-circle automated diffractometer and MoKα radiation (graphite monochromator). The equivalent pairs *hkl* and $hk\bar{l}$ were measured using ω scan mode in the 2θ range 3 to 60° or 70°. After correcting the X-ray intensities for Lorentz, polarization and absorption factors (North et al. 1968), the values for the equivalent pairs were averaged and the site occupancies were refined in the space group *Pbca*, along with a scale factor, extinction coefficient and atomic positional and anisotropic thermal parameters. The total number of non-equivalent reflections varied between 900 and 1800. The scattering factors were taken from the International Tables for X-ray Crystallography (1974) and Tokonami (1965).

In the refinements using ionic scattering factors, Fe, Mg, Ca, Cr, Na, Al and Ti were considered to have the respective formal charges, whereas Si and O were considered to be in the partly ionized states of 2.5+ and 1.5−, respectively. It was assumed, as is the common practice (e.g., Domeneghetti et al. 1985; Ganguly et al. 1994; Yang and Ghose 1994) that ^{VI}Al, Cr, Fe^{3+} and Ti were confined to the M1 site, Ca and Na to the M2 site, and that Mn^{2+} partitioned between the two octahedral sites in the same way as Fe^{2+} (Hawthorne and Ito 1978). Structure and site occupancy refinements were carried out using different weighting schemes, scattering factors and two different programs, SHELXL-93 and RFINE90. The results are summarized in Tables 1–2 for the crystals ST77, SJN 23 and 25, JS and HO28. The stated uncertainties (1σ) of the site occupancies are those due *only* to the statistical errors of the structural data. The possible effects of the errors of the bulk composition are discussed later.

Table 1 Conditions of annealing experiments and results of site occupancy determinations for the samples ST77 (Fs_{15}), SJN23 (Fs_{14}), SJN25 (Fs_{14}) and H028 (Fs_{49}) using the programs RFINE90 and SHELXL-93, atomic and ionic scattering factors and individual weights. The *numbers within the parentheses* are the estimated standard deviations (in the *right* justified form) arising from those in the structural data

T °C Experiment type Time (h)	Program	Scattering factor	No. Ind. Refl.[a]	GOF[b]	Rw%	X_{Fe^*}(M1)	X_{Fe^*}(M2)	$-\ln k_D^*$	$\sigma(\ln k_D^*)$
SJN(Fs_{14})									
700									
Ordering	SHELXL	Ionic	1830	1.036	6.43	0.0326 (22)	0.2666 (22)	2.3784	(658)
240	RFINE	Ionic	1532	1.090	2.50	0.0331 (12)	0.2673 (12)	2.3662	(352)
750									
Ordering	SHELXL	Ionic	1835	1.074	5.87	0.0381 (16)	0.2611 (15)	2.1884	(410)
40.65	RFINE	Ionic	1604	1.020	2.00	0.0375 (9)	0.2630 (9)	2.2148	(266)
800									
Disordering	SHELXL	Ionic	1842	1.169	5.39	0.0413 (18)	0.2578 (18)	2.0873	(427)
2.1	RFINE	Ionic	1599	1.000	1.90	0.0420 (9)	0.2583 (9)	2.0724	(207)
SJN25 (Fs_{14})									
750									
Disordering	SHELXL	Ionic	1674	1.007	5.66	0.0362 (25)	0.2619 (27)	2.2457	(680)
40.65	RFINE	Ionic	1224	0.970	2.90	0.0373 (15)	0.2608 (15)	2.2089	(392)
ST77 (Fs_{15})									
700	SHELXL	Ionic	1235	0.979	4.45	0.0380 (17)	0.2872 (19)	2.3224	(495)
Disordering	SHELXL	Atomic	1223	0.963	6.36	0.0362 (27)	0.2890 (24)	2.3816	(725)
827.04	RFINE	Ionic	965	0.970	1.20	0.0382 (9)	0.2874 (9)	2.3179	(244)
700	SHELXL	Ionic	1235	0.995	3.99	0.0359 (18)	0.2892 (16)	2.3912	(520)
Ordering	SHELXL	Atomic	1235	1.095	4.89	0.0358 (28)	0.2894 (25)	2.3951	(768)
456	RFINE	Ionic	954	0.910	1.10	0.0366 (9)	0.2890 (9)	2.3702	(246)
800	SHELXL	Ionic	1227	1.004	4.79	0.0474 (20)	0.2778 (21)	2.0452	(432)
Disordering	SHELXL	Atomic	1227	1.081	6.88	0.0467 (28)	0.2785 (28)	2.0643	(583)
36	RFINE	Ionic	969	0.980	1.20	0.0488 (10)	0.2768 (10)	2.0096	(194)
800	SHELXL	Ionic	1232	0.998	4.44	0.0474 (17)	0.2778 (20)	2.0452	(423)
Ordering	SHELXL	Atomic	1239	1.085	6.31	0.0483 (28)	0.2769 (30)	2.0209	(573)
72	RFINE	Ionic	949	0.960	1.20	0.0483 (10)	0.2773 (10)	2.0229	(204)
900	SHELXL	Ionic	1233	1.013	4.21	0.0544 (18)	0.2707 (17)	1.8644	(336)
Disordering	SHELXL	Atomic	1233	1.075	6.09	0.0544 (28)	0.2709 (27)	1.8654	(504)
30	RFINE	Ionic	970	0.940	1.10	0.0564 (9)	0.2691 (9)	1.8180	(172)
900	SHELXL	Ionic	1228	1.015	4.06	0.0550 (19)	0.2702 (19)	1.8502	(249)
Ordering	SHELXL	Atomic	1228	1.075	5.70	0.0557 (28)	0.2695 (29)	1.8333	(494)
168	RFINE	Ionic	937	0.910	1.10	0.0561 (10)	0.2695 (10)	1.8257	(161)
1000	SHELXL	Ionic	1263	0.991	4.28	0.0638 (17)	0.2615 (19)	1.6479	(286)
Disordering	SHELXL	Atomic	1236	1.072	6.19	0.0649 (27)	0.2603 (29)	1.6234	(416)
10	RFINE	Ionic	944	0.930	1.20	0.0633 (9)	0.2623 (9)	1.6604	(153)
HO28 (Fs_{49})									
550	SHELXL	Ionic	1254	1.040	4.06	0.2263 (21)	0.8026 (26)	2.6319	(181)
Disordering	SHELXL	Atomic	1254	1.030	4.12	0.2309 (24)	0.7979 (30)	2.5765	(197)
1224	RFINE	Ionic	1015	0.980	1.00	0.2278 (10)	0.8010 (10)	2.6133	(68)
550	SHELXL	Ionic	1254	1.007	3.94	0.2332 (20)	0.7954 (25)	2.5481	(166)
Ordering	SHELXL	Atomic	1253	1.070	5.25	0.2356 (27)	0.7930 (32)	2.5201	(211)
2640	RFINE	Ionic	1035	0.960	1.00	0.2339 (10)	0.7949 (10)	2.5411	(63)
650	SHELXL	Ionic	1255	1.112	4.82	0.2606 (25)	0.7675 (31)	2.2371	(187)
Disordering	SHELXL	Atomic	1253	1.166	5.74	0.2606 (32)	0.7676 (37)	2.2377	(225)
30	RFINE	Ionic	996	0.980	1.00	0.2591 (10)	0.7692 (10)	2.2545	(57)
650	SHELXL	Ionic	1252	1.002	3.77	0.2607 (19)	0.7675 (23)	2.2366	(140)
Ordering	SHELXL	Atomic	1252	1.099	5.13	0.2610 (27)	0.7672 (31)	2.2333	(187)
45	RFINE	Ionic	1024	0.960	1.00	0.2605 (10)	0.7678 (10)	2.2393	(56)
750	SHELXL	Ionic	1256	1.000	3.89	0.2891 (21)	0.7385 (23)	1.9379	(125)
Disordering	SHELXL	Atomic	1256	1.071	5.15	0.2891 (28)	0.7385 (30)	1.9379	(167)
5.16	RFINE	Ionic	1006	0.960	1.10	0.2856 (10)	0.7422 (10)	1.9743	(58)
750	SHELXL	Ionic	1255	1.002	4.27	0.2881 (24)	0.7397 (24)	1.9490	(133)
Ordering	SHELXL	Atomic	1255	1.069	5.49	0.2873 (30)	0.7404 (31)	1.9566	(170)
15	RFINE	Ionic	1019	1.060	1.10	0.1413 (11)	0.7405 (11)	2.8531	(156)
850	SHELXL	Ionic	1256	1.001	4.47	0.3104 (25)	0.7166 (27)	1.7259	(140)
Disordering	SHELXL	Atomic	1256	1.065	5.87	0.3125 (32)	0.7148 (33)	1.7073	(171)
14	REFINE	Ionic	982	0.970	1.10	0.3101 (11)	0.7173 (11)	1.7308	(56)

[a] (*No. Ind. Refl.* number of independent reflections)
[b] (*GOF* goodness of fit)

Table 2 Conditions of annealing experiments and results of site occupancy determinations for the sample JS (Fs_{23}) using the programs RFINE90 and SHELXL-93, ionic scattering factors and individual (*I*) and unit (*U*) weights. The *number within the parentheses* are the estimated standard deviations (in the *right* justified form) arising from those in the structural data. The X-ray data are from Molin et al. (1991)

T °C Experiment type Time (hours)	Program (*weighting*)	Scattering factor	No. Ind. Refl.[a]	GOF[b]	R%	X_{Fe^*}(M1)	X_{Fe^*}(M2)	$-\ln k_D^*$	$\sigma(\ln k_D^*)$
700									
Disordering	SHELXL (*I*)	Ionic	1227	1.063	5.58	0.0828 (25)	0.4151 (24)	2.0620	(307)
700	RFINE (*I*)	Ionic	1004	0.990	2.00	0.0844 (14)	0.4134 (14)	2.0341	(176)
	RFINE (*U*)	Ionic	978	2.020	3.20	0.0827 (33)	0.4089 (33)	2.0377	(414)
700									
Ordering	SHELXL (*I*)	Ionic	1235	1.065	5.77	0.0835 (24)	0.4134 (26)	2.0495	(295)
833.33	RFINE (*I*)	Ionic	1053	1.090	1.90	0.0801 (20)	0.4177 (20)	2.1088	(288)
	RFINE (*U*)	Ionic	1040	2.080	2.80	0.0805 (28)	0.4173 (28)	2.1017	(368)
750									
Disordering	SHELXL (*I*)	Ionic	1233	1.089	5.71	0.0871 (27)	0.4106 (28)	1.9881	(314)
366.67	RFINE (*I*)	Ionic	1064	1.110	1.90	0.0872 (12)	0.4105 (12)	1.9864	(283)
	RFINE (*U*)	Ionic	1050	2.130	2.90	0.0868 (28)	0.4109 (28)	1.9931	(352)
750									
Ordering	SHELXL (*I*)	Ionic	1232	1.257	5.99	0.0863 (28)	0.4114 (30)	2.0015	(340)
583.33	RFINE (*I*)	Ionic	1051	1.020	1.80	0.0884 (12)	0.4093 (12)	1.9665	(259)
	RFINE (*U*)	Ionic	1034	2.090	2.80	0.0888 (28)	0.4089 (28)	1.9599	(341)
800									
Disordering	SHELXL (*I*)	Ionic	1232	1.091	5.58	0.0946 (30)	0.4030 (31)	1.8657	(323)
191.67	RFINE (*I*)	Ionic	1043	1.040	1.80	0.0951 (13)	0.4025 (13)	1.8578	(257)
	RFINE (*U*)	Ionic	1018	2.130	2.90	0.0958 (29)	0.4018 (29)	1.8468	(330)
800									
Ordering	SHELXL (*I*)	Ionic	1233	1.082	5.01	0.0972 (21)	0.4003 (22)	1.8245	(223)
166.67	RFINE (*I*)	Ionic	1036	0.970	1.70	0.0945 (12)	0.4030 (12)	1.8669	(211)
	RFINE (*U*)	Ionic	1003	2.030	2.75	0.0940 (28)	0.4036 (28)	1.8753	(320)
900									
Disordering	SHELXL (*I*)	Ionic	1233	1.093	5.43	0.1090 (24)	0.3883 (27)	1.6465	(244)
25	RFINE (*I*)	Ionic	1041	1.040	1.90	0.1110 (12)	0.3862 (12)	1.6173	(121)
	RFINE (*U*)	Ionic	1011	1.980	2.75	0.1108 (28)	0.3865 (28)	1.6205	(273)
900									
Ordering	SHELXL (*I*)	Ionic	1235	1.042	5.04	0.1079 (22)	0.3894 (23)	1.6625	(216)
50	RFINE (*I*)	Ionic	1031	0.980	1.70	0.1077 (13)	0.3896 (13)	1.6655	(132)
	RFINE (*U*)	Ionic	1013	1.940	2.65	0.1077 (27)	0.3896 (27)	1.6655	(270)
1000									
Disordering	SHELXL (*I*)	Ionic	1232	1.053	5.87	0.1209 (28)	0.3761 (30)	1.4778	(250)
16.67	RFINE (*I*)	Ionic	1033	0.980	1.80	0.1207 (13)	0.3763 (13)	1.4805	(192)
	RFINE (*U*)	Ionic	1014	2.190	2.95	0.1210 (30)	0.3761 (30)	1.4769	(271)
1000									
Ordering	SHELXL (*I*)	Ionic	1234	1.039	5.47	0.1258 (26)	0.3711 (27)	1.4111	(221)
31.67	RFINE (*I*)	Ionic	1014	0.940	1.70	0.1235 (12)	0.3734 (21)	1.4420	(106)
	RFINE	Ionic	984	2.170	2.80	0.1223 (29)	0.3747 (29)	1.4587	(262)

[a] (*No. Ind. Refl.* number of independent reflections)
[b] (*GOF* goodness of fit)

Program RFINE 90

This is an updated version of the widely used program RFINE4 (Finger and Prince 1975), as modified by L. Finger. The program recommends the use of Fo. Structure refinements were carried out using ionic scattering factors and both weighted and unweighted nonequivalent reflections. The Fo values are weighted by $(1/\sigma')^2$ so that the weighted difference between the observed and calculated intensities, $\Delta F_i/\sigma'$, has a normal distribution with mean 0 and variance 1. The σ' is derived from $\sigma(Fo)_i$ given by the counting statistics by using a normal probability plot. The rationale behind this approach has been discussed in the International Tables for X-Ray Crystallography, vol. IV (1974) and by Abrahams and Keve (1971). This program can be used directly to calculate the site occupancies using fixed bulk compositions.

Program SHELXL-93

SHELXL-93 (Sheldrick 1993) is one of the most widely used crystallographic programs. The structure refinements were carried out using Fo^2, as recommended by the program, and all nonequivalent reflections, which

Table 3 Initial and adjusted (*adj.*) composition of orthopyroxene crystals ST77, HO28, SJN23 and SJN24. No adjustment was required to the initial composition of JS

	ST77	esd[a]	ST77 adj	JS	esd	JS adj	HO28	esd	HO28 adj	SJN23	esd	SJN23 adj	SJN25	esd	SJN25 adj
Oxide %															
SiO_2	56.61	(17)	56.38	54.29	(15)	54.29	51.01	(25)	50.96	56.96	(13)	56.44	56.89	(32)	56.35
Al_2O_3	0.23	(1)	0.37	1.08	(4)	1.08	0.89	(2)	0.92	0.28	(1)	0.37	0.28	(1)	0.47
TiO_2	0.01	(1)	0.00	0.11	(1)	0.11	0.11	(1)	0.13	0.03	(1)	0.62	0.02	(1)	0.19
Cr_2O_3	0.60	(2)	0.55	0.84	(3)	0.84	0.01	(1)	0.02	0.69	(3)	31.80	0.71	(3)	0.70
MgO	31.21	(12)	31.44	26.66	(12)	26.66	16.57	(16)	16.40	31.95	(11)	9.33	32.08	(1)	31.83
FeO	10.25	(8)	10.33	15.15	(11)	15.15	30.67	(16)	30.22	9.34	(12)	0.60	9.39	(25)	9.32
MnO	0.54	(3)	0.55	0.46	(2)	0.46	0.44	(6)	0.43	0.60	(4)	0.60	0.60	(8)	0.59
CaO	0.36	(1)	0.38	1.39	(7)	1.39	0.90	(2)	0.90	0.60	(2)	0.22	0.60	(3)	0.60
Na_2O	0.02	(1)	0.00	0.01	(1)	0.01	0.01	(1)	0.00	0.10	(1)	0.00	0.01	(1)	0.01
Total	99.83		100.00	99.99		99.99	100.61		99.98	100.55		99.98	100.58		100.06
a.p.f.u															
Si	1.9906	(30)	1.9848	1.9630	(30)	1.9630	1.9699	(50)	1.9749	1.9862	(19)	1.9840	1.9848	(0)	1.9807
Al	0.0092	(30)	0.0152	0.0460	(30)	0.0460	0.0405	(10)	0.0421	0.0138	(50)	0.0160	0.0151	(40)	0.0193
Ti	0.0000	(0)	0.0000	0.0030	(10)	0.0030	0.0032	(10)	0.0039	0.0005	(4)	0.0001	0.0007	(5)	0.0005
Cr	0.0152	(10)	0.0152	0.0240	(10)	0.0240	0.0003	(10)	0.0006	0.0184	(9)	0.0173	0.0196	(6)	0.0194
Mg	1.6450	(40)	1.6500	1.4370	(40)	1.4370	0.9521	(60)	0.9472	1.6684	(42)	1.6665	1.6685	(100)	1.6653
Fe^{2+}	0.3042	(23)	0.3042	0.4580	(60)	0.4580	0.9881	(80)	0.9794	0.2754	(31)	0.2743	0.2738	(31)	0.2735
Mn	0.0160	(10)	0.0163	0.0140	(10)	0.0140	0.0144	(10)	0.0143	0.0180	(9)	0.0179	0.0177	(9)	0.0177
Ca	0.0140	(10)	0.0143	0.0540	(30)	0.0540	0.0376	(10)	0.0375	0.0225	(7)	0.0225	0.0226	(6)	0.0226
Na	0.0000	(0)	0.0000	0.0010	(10)	0.0010	0.0007	(10)	0.0002	0.0012	(5)	0.0015	0.0009	(6)	0.0010
Total	3.9942		4.0000	4.0000		4.0000	4.0068		4.0001	4.0044		4.0001	4.0037		4.0000
Charge	11.9940		12.0000	12.0010		12.0010	11.9999		12.0003	12.0132		12.0002	12.0122		12.0001
Al(T)[b]	0.0092		0.0152	0.0370		0.0370	0.0301		0.0251	0.0138		0.0160	0.0151		0.0193
Al(M)[b]	0.0000		0.0000	0.0090		0.0090	0.0104		0.0170	0.0000		0.0000	0.0000		0.0000
d(chrg(M))[c]	0.0152		0.0152	0.0380		0.0380	0.0164		0.0252	0.0182		0.0160	0.0201		0.0194
d(M−T)[d]	0.0060		0.0000	0.0010		0.0010	−0.0137		0.0001	0.0044		0.0000	0.0050		0.0001
M-cations	1.9944		2.0000	2.0000		2.0000	2.0068		2.0001	2.0044		2.0001	2.0038		2.0000

[a] (*esd* estimated standard deviation from the mean of the spot analyses in the *right* justified form)
[b] (*Al(T)* Al in T site, *Al(M)* Al in M site)
[c] (*d[chrg(M)]* excess positive charge in M site due to the substitution for 2+ cations)
[d] (*d(M−T)* difference between the charge excess in M site and the charge deficiency in T site)

were weighted by the program according to a built in scheme with adjustable parameters. However, our data did not require the use of more than two (a and b) adjustable parameters. A small number of reflections were occasionally removed from the data set from those identified by the program as possible outliers, and the refinements were repeated. This improved the goodness of fit (GOF), but had no significant effect on the final site occupancy values. The distribution of $\Delta Fo/\sigma$ has been analyzed separately in several cases, and found to closely approximate a normal distribution. The cation distributions were calculated by combining the results of structure refinements and crystal-chemically constrained bulk compositional data for the individual crystals. However, unlike RFINE 90 this program does not permit one to restrict the bulk composition of a crystal to an absolutely fixed value. Thus, the cation distributions were calculated through a minimization program MINUIT (James and Roos 1975). The quantity minimized was $[(Q_{obs} - Q_{calc})/\sigma(Q_{obs})]^2$, where Q stands for the structural parameters. The program was not allowed to vary the bulk composition. The chemical parameters were the atomic fractions of the elements whereas the structural parameters were the mean atomic numbers (m.a.n.) at the M1 and M2 sites. The m.a.n. of a given site was determined by refining the crystal as a binary solid solution of Mg and Fe^{2+} components. This procedure, which has been employed in many earlier studies (e.g., Molin et al. 1991, 1994a, b; Ganguly and Domeneghetti 1996) implicitly assumes that the scattering factor of a nonbinary component is an electron conservative linear combination of those of Fe^{2+} and Mg. While this is not exactly valid, the error introduced by this assumption is not significant for orthopyroxene which has very small amounts of nonbinary components.

We carried out two sets of refinements for all the annealing data for the samples ST77 and HO28 using both ionic and atomic scattering factors (Table 1). Although the site occupancy values were not significantly different except for the sample ST77 disordered at 700 °C (Table 1: ST77/700-Disordering), the use of ionic scattering factor always resulted in significantly better GOF and $R_w(Fo^2)$ in the structure refinement, and slightly smaller estimated standard deviation of the site occupancy data.

Microprobe analyses

The microprobe analyses were carried out using 15 kV accelerating voltage, 20–25 nA beam current, and

counting times of 20 s at the peak and 20 s at the background for JS, and 50 s at the peak and 50 s at the background for ST77, SJN 23 and 25, and HO28. In order to improve the accuracy of the analyses, we used mostly *synthetic standards of stoichiometric minerals* so that the compositions of the standards are known exactly. The standards used were as follows: synthetic diopside or synthetic ferrosilite for Si, synthetic corundum or synthetic pyrope for Al, synthetic diopside or synthetic grossularite for Ca, natural albite or synthetic jadeite for Na, synthetic $CaTiO_3$ or synthetic $MnTiO_3$ for Ti, synthetic chromite for Cr, synthetic $MnTiO_3$ or synthetic spessartine for Mn, natural olivine or synthetic ferrosilite for Fe, synthetic diopside or synthetic enstatite for Mg. When two different standards are listed for the same element, the first one refers to the analyses of JS, and the second one to those of SJN(23 and 25), ST77 and HO28. The use of two different sets of standards was due to the fact that the analyses were carried out at two different microprobe facilities, one at the University of Padova (Cameca/Camebax) and the other at the University of Arizona (Cameca Superprobe SX50). Each crystal was found to be homogeneous in composition within the precision of the microprobe data. Only those spot analyses that had oxide totals of 100 ± 1 were selected and averaged (Table 3). These represent 55 spot analyses for JS, 41 for SJN 23, 23 for SJN25, 81 for ST77 and 48 for HO28.

Determination of statistically most probable bulk compositions

Ganguly et al. (1994) noted that the ordering states of orthopyroxene crystals separated from the same rock, as determined with bulk compositional constraints imposed by the average of a large number of microprobe spot analyses (oxide totals of 100 ± 1), sometimes differed significantly. However, much of these differences disappeared when the average composition of each crystal was readjusted to satisfy the following crystal chemical constraints for six oxygens per formula unit: (1) the total positive charge = 12.000; (2) the total occupancy of T (tetrahedral) sites = the total occupancy of M (octahedral) site = 2.000. Only those data were accepted in which the composition of a crystal did not require readjustment beyond the 2σ limit from its average composition to satisfy the above constraints. In this work, we have made these adjustments using a computer program based on the mathematical technique developed by Dollase and Newman (1984), which permits finding the stoichiometrically constrained point that is nearest to the measured point in the *n*-dimensional compositional space. This is achieved by constrained minimization of the quantity U with respect to X_i, using the standard procedure of Lagrangian multipliers, where $U = \sum_{i=1}^{n}(Y_i - X_i)^2/\delta_i^2$, Y_i being the measured concentration of an element with a standard deviation σ_i and X_i is its concentration on the stoichiometrically constrained surface. Initial estimates of Al(IV) and Al(VI), treated as the respective measured values, were made according to Al(IV) = 2 − Si, so that $\sigma_{Al(IV)} = \sigma_{Si}$, and Al(VI) = Al($t$) − Al(IV), where t stands for total, so that $\sigma_{Al(VI)} = (\sigma^2_{Al(t)} + \sigma^2_{Al(IV)})^{1/2}$.

The average and the adjusted analyses of each crystal are summarized in Table 3. For both ST77 and JS, the adjusted compositions are within 1σ of the average analyzed compositions. Thus, there was no need to invoke the presence of Fe^{3+} in these samples. This is consistent with the fact that these samples were separated from meteorites which crystallized at f_{O_2} conditions within the field of metallic iron. For the terrestrial granulite sample HO28, the difference between the adjusted and initial compositions of only Fe^{2+} and Al(VI) slightly exceeded the 1σ values of the respective initial compositions. We assumed all Fe to be in the divalent state also for this sample, especially in as much as the samples were annealed in the presence of Fe-FeO buffer prior to the microprobe analyses. It is emphasized, however, that the site occupancy data are very sensitive to the errors in the estimation of Fe^{3+}. For example, if we assume that 1 mol% of the total iron in HO28 is Fe^{3+}, then the $\ln k_{D^*}$, as defined below, would be lower by ~ 0.10.

Results and discussion of refinement strategies

The site occupancy data were used to calculate the intracrystalline distribution coefficient, k_D^*, which is defined as the ratio $(Fe^*/Mg)^{M1}/(Fe^*/Mg)^{M2}$, according to the homogeneous exchange equilibrium

$$Fe^*(M2) + Mg(M1) = Fe^*(M1) + Mg(M2) \quad , \qquad (a)$$

where Fe^* represents $Fe^{2+} + Mn^{2+}$, as these were treated as one component in the structure refinement. (Following earlier practices, e.g., Ganguly et al. 1994; Ganguly and Domeneghetti 1996, we use the symbol k_D for the *intra*crystalline distribution coefficient in order to distinguish it from the conventional symbol of K_D used to designate *inter*crystalline distribution coefficient.) The k_D^* versus 1/T relation for each crystal (SJN23, SJN25, ST77, HO28 and JS), obtained from each type of refinement procedure, is illustrated in Fig. 1a, b and c. The orientation of the triangles indicates the direction of approach of equilibrium k_D^*.

From the data summarized in Tables 1 and 2, and illustrated in Fig. 1a–c, the following observations can be made:

1. Overall, the site occupancy values obtained from the different refinement strategies were mutually compatible within their estimated standard deviations (esd). However, the esds of site occupancies retrieved from the weighted refinements were smaller by a factor of 2–3 than those from unweighted refinements on selected reflections [$I/\sigma(I) > 3$–5], even when the number of reflections was kept the same in the two types of refinements.

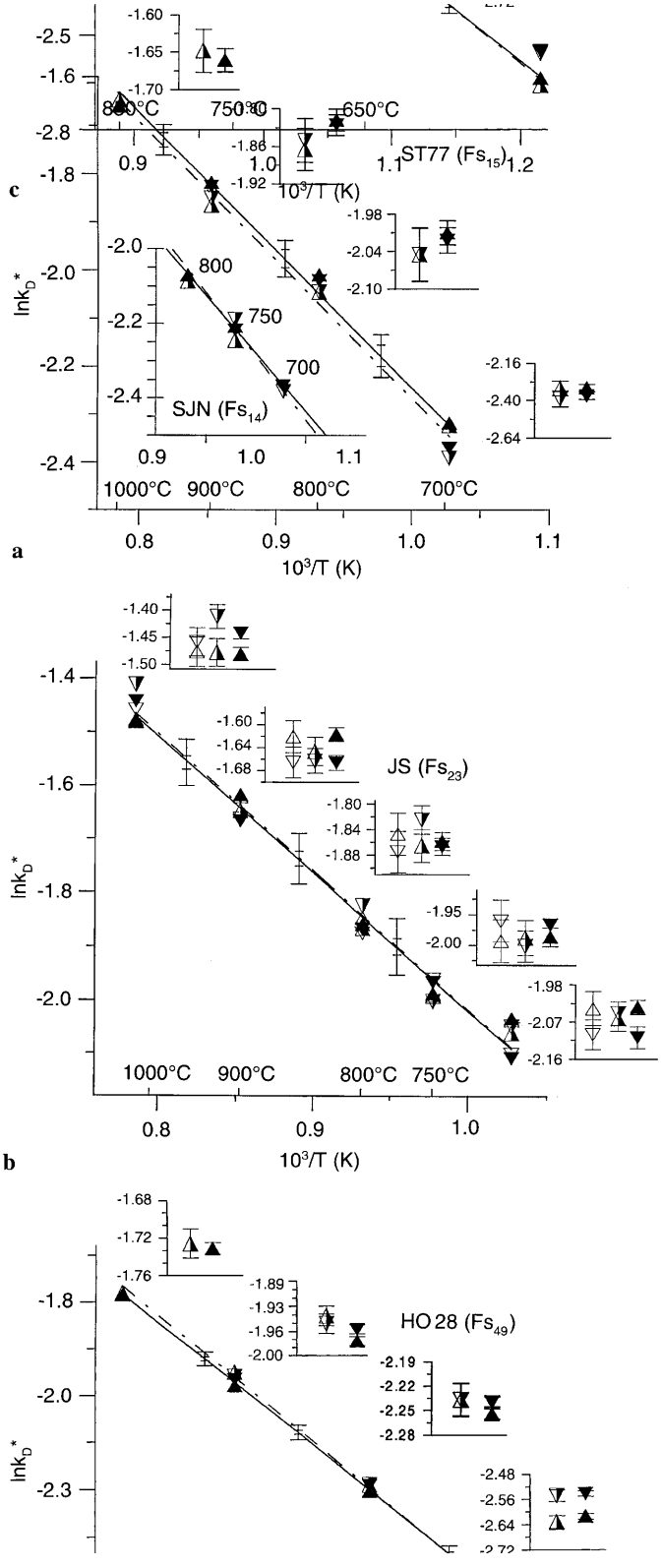

◀

Fig. 1 a–c Variation of the intracrystalline Fe*-Mg ($Fe^* = Fe^{2+}$ + Mn) distribution coefficient, k_D^*, as a function of temperature for the orthopyroxene samples investigated in this study: **a** ST77 (Fs_{15}) and SJN (Fs_{14}) in *main* figure and in the *large inset*, respectively; **b** JS (Fs_{23}); **c** HO28 (Fs_{49}). For clarity, the results obtained from the different structure refinement strategies (see text) are also shown in enlarged scales *above* the regression lines, except for SJN. *Half-filled triangles and hyphenated lines*: Data from SHELXL-93 and the corresponding least squared fits; *filled triangles and solid lines*: Data from RFINE90 and the corresponding least squared fits. In Fig. 1b the *open triangles* in the insets refer to the results from unweighted refinements from RFINE90. *Upward* and *downward pointing* orientations of the *triangles* correspond to the direction of change of k_{D^*} during annealing experiments. The error *bars* in the *insets* indicate $\pm 1\sigma$ uncertainty of the $\ln k_{D^*}$ values arising from those in the structural data. The *smaller* error bars on the $\ln k_D^*$ versus $1/T$ calibrations indicate $\pm 1\sigma$ uncertainties arising from the errors of the structural data alone (RFINE90); the *larger* ones represent the probable combined errors of structural (RFINE90) and chemical data (see text). For HO28 (**c**), steady state was not achieved in the ordering experiment at 550 °C (*downward pointing triangle*). This datum was excluded from the regression

2. Compared to the atomic scattering factor, the use of ionic scattering factor yields better goodness of fit (GOF) and weighted agreement index (R_w), and smaller standard deviation on the site occupancy data.
3. Kroll et al. (1997) concluded that the use of unit weight leads to significantly more disordered site occupancy compared to that determined with individual weights. Our results do not support this as a generally valid observation (Table. 2).

Effect of uncertainty of the bulk composition calculation on the site occupancy refinement

We have derived above the site occupancies according to the statistically most probable bulk compositions of the crystals that can be derived from the microprobe data, but have not accounted for the effect of error of microprobe analyses on the site occupancies. This is a difficult task, which would require finding the sets of compositions on the stoichiometrically constrained surface in the *n*-dimensional compositional space that could result from the random variation of the concentration of each element within the errors of the microprobe analyses, and finding the site occupancies corresponding to each set. Work is currently in progress to address this problem. Meanwhile, we try to develop an approximate feeling for the effect of bulk compositional uncertainty on the site occupancies by selecting a few extreme compositions within the (1σ) error limits of the microprobe analyses that satisfy the crystal chemical constraints, and determining the site occupancies for each of these compositions for a given crystal. Since we are dealing with multicomponent crystals, the variation of the concentration of one cation, say Fe^{2+}, may be charge-compensated by a variety of changes in the concentration of other cations. However, because Fe^{2+} and Mg are the major components, we have restricted

our analyses to the complementary variation of these cations within the 1σ limits of their microprobe analyses, and to the determination of the corresponding site occupancies using RFINE90. This exercise suggests that accounting for the errors in the microprobe data would expand the standard deviations of the site occupancies given by RFINE90 by a factor of ~2 for S77 and 3–4 for JS and HO28.

Comparison with the method of Kroll et al. (1997)

Kroll et al. (1997) published a new site occupancy refinement strategy, which they referred to as 'Bivariate Analysis'. They found that the site occupancies determined in an orthopyroxene crystal (Fs_{11}) from the Acapulcoite meteorite (ALHA81261) depended on the subjectively chosen $\Delta F/\sigma(Fo)$ limits for the rejection of the outliers for both high order and low order reflections, and also on the $\sin\theta/\lambda$ limits of truncation of these reflections. Thus, they recommended separate determination of the weighted average of: (1) the site occupancies in each subset of the high order reflections (HOT); (2) those in each subset of low order reflections (LOT), and further averaging these HOT and LOT averages according to their respective weights.

In their LOT analyses, Kroll et al. (1997) assumed isotropic vibrations of the M1 and M2 atoms and refined the structure with a fixed ratio of B(M2)/B(M1), which was varied stepwise, to remove the observed correlation on the displacement parameters. The X-ray data were weighted by $1/\sigma^2(Fo)$, where σ represents the larger of the σ value based on the counting statistics and that derived from the intensity variation of the equivalent reflections. This procedure yielded Fe(M2) = 0.189(2), the parenthetical number indicating the standard deviation in the right justified form (i.e. ±0.002). More recently, this procedure has been further refined (H. Kroll, personal communication), using a new weighting scheme and anisotropic thermal vibrations with fixed ratio of $B_{ij}(M2)/B_{ij}(M1)$. The modified procedure yields Fe(M2) = 0.188(1) for the orthopyroxene from ALHA81261.

In order to compare the results of the refinement strategies used in this work with those of Kroll et al. (1997) and its subsequent modification, we obtained the X-ray data of ALHA81261 orthopyroxene crystal (H. Kroll, personal communication) and determined the site occupancies. The results are as follows: Fe(M2) = 0.186(2) for SHELXL-93 and 0.188(1) for RFINE90, which are in excellent agreement with those of H. Kroll et al. (personal communication).

Thermodynamic analysis

Distribution coefficient as a function of temperature and composition

A simple thermodynamic functional form that is most commonly used to express the temperature and compositional dependence of the intracrystalline distribution coefficient, k_D, in a binary system is given by

$$\ln k_D = -\frac{\Delta H^0}{RT} + \frac{\Delta S^0}{R} + \frac{W^{M2}}{RT}\left(1 - 2X_{Fe}^{M2}\right) - \frac{W^{M1}}{RT}\left(1 - 2X_{Fe}^{M1}\right) \quad (1)$$

where W^{M2} and W^{M1} are *simple mixture* type interaction parameters, which not only reflect the interactions of Fe and Mg within the individual sites, but also across the sites. The latter can be identified as the classic Bragg and Williams (BW) interaction parameter so that $W^{M2} = W^{M2}$ (site) + W(BW), and similarly for W^{M1} (Thompson 1970; Sack 1980; Ganguly 1982). However, it is not possible to determine both intra- and inter-site interaction parameters from the site occupancy data alone. The derivation of the above expression is given by Sack (1980) and Ganguly (1982) using different approaches, clarifying the nature of the W parameters. The use of Eq. (1) to treat the orthopyroxene crystals is justified as these are either binary (synthetic samples) or quasibinary under the assumption that Fe and Mn behave similarly, in which case $X_{Fe} = X_{Fe^*} = Fe^*/(Fe^* + Mg)$ in each site and $k_D = k_{D^*}$.

An alternative expression for the temperature and compositional dependence of k_D has been derived by Kroll et al. (1997) in terms of an order parameter Q_t and bulk composition, X_{Fe}, which is as follows.

$$\ln k_D = -\frac{\Delta H^0}{RT} + \frac{\Delta S^0}{R} + \frac{\left(L^{M1} - L^{M2}\right)}{RT}X_{Fe} + \frac{\left[\Delta G_{rec}^0 - \left(L^{M1} + L^{M2}\right)\right]}{RT}Q_t \quad (2)$$

where $Q_t = X_{Fe}^{M2} - X_{Fe}^{M1}$ (Thompson, 1969), X_{Fe} = Fe/(Fe + Mg), and similarly for X_{Fe}^{M1} and X_{Fe}^{M2}, ΔG_{rec}^0 is the reciprocal exchange free energy [$G^0(Fe^{M2}Mg^{M1}Si_2O_6) + G^0(Mg^{M2}Fe^{M1}Si_2O_6) - G^0(Fe^{M2}Fe^{M1}Si_2O_6) - G^0(Mg^{M2}Mg^{M1}Si_2O_6)$], and L-s represent the intra- or within-site interaction parameters, and are the same as W(site) terms defined above. Also, $\Delta G_{rec}^0 = -2W(BW)$ (Ganguly 1986). As demonstrated by Kroll et al. (1997), Eqs. (1) and (2) are exactly equivalent for minerals in which the two types of sites occupied by the exchanging atoms are present in equal multiplicity (e.g., binary Fe-Mg orthopyroxene), but are nonequivalent when this condition is significantly violated (e.g., clinopyroxene). For the first case, we have $W^{M1} - W^{M2} = L^{M1} - L^{M2}$, and $(W^{M1} + W^{M2}) = \Delta G^0 - (L^{M1} + L^{M2})$, which permit determination of the constant coefficients required to express $\ln k_D$ as a function of composition according to Eq. 2 from those in Eq. 1, and vice versa.

Our initial objective has been to find an expression of k_{D^*} as a function of temperature and composition that can be used to calculate the closure temperature, T_C, of cation ordering in natural samples for the purpose of cooling rate calculations. To this end, we explore below the effectiveness of the functional form of Eq. 1 to express the experimental data on the temperature and

compositional dependence of k_{D^*}, as determined in this study and by other workers using single crystal X-ray data. In the latter group, we incorporate the results of site occupancy determination of: (1) a crystal (Fs_{11}) from an Antarctic meteorite sample (ALHA 81261) by Lueder (1995; H. Kroll, personal communication); (2) a crystal (Fs_{23}) from Johnstown meteorite (sample JS) as determined above using the single crystal X-ray data of Molin et al. (1991); (3) synthetic crystals (Fs_{19} and Fs_{51}) by Schlenz (1995); (4) synthetic crystals (Fs = 0.25, 0.39, 0.51, 0.75, 0.83) by Yang and Ghose (1994). The synthetic crystals are restricted to the Fe-Mg binary compositions. These data, along with those from the present study, are illustrated in Fig. 2 as two isothermal $\ln k_D^*$ versus X_{Fe} plots at 850 and 1000 °C. Some of the data represent interpolated values. The data of Lueder (1995), as cited in Kroll et al. (1997) are erroneous. The ones shown in Fig. 2 are the corrected values (H. Kroll personal communication). Yang and Ghose (1994) noted disagreement between their data for Fs_{25} with those of Molin et al. (1991) for the sample JS (Fs_{23}). However, the revised results for JS do not show any significant disagreement with those of Yang and Ghose (1994) (Fig. 3).

We decided not to mix the results of earlier Mössbauer data on site occupancy (Saxena and Ghose 1971; Anovitz et al. 1988) with those from single crystal structure refinement, since in the Mössbauer data ($1-X_{Fe}$) was equated to X_{Mg} in each site of natural *non binary* orthopyroxene crystals, and also because there may be some intrinsic differences between the results of single crystal and Mössbauer techniques, especially when the latter fails to *properly* account for the effect of sample

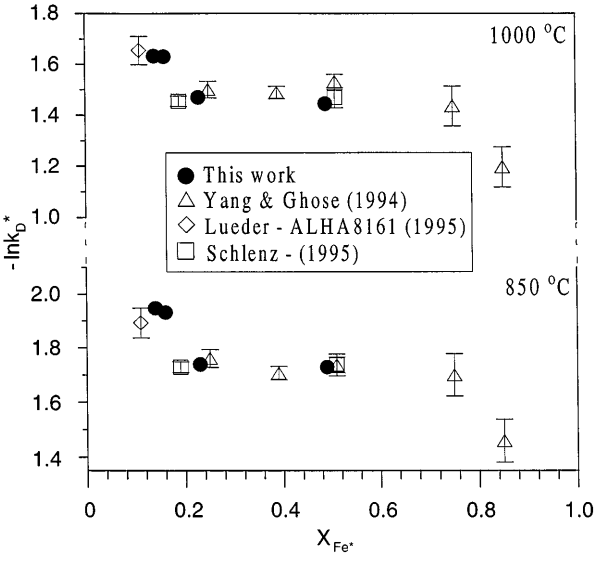

Fig. 2 Comparison of $\ln k_{D^*}$ versus X_{Fe} of orthopyroxenes determined recently by single crystal structure refinements at two selected temperatures, 1000 and 850 °C. The data for Schlenz (1995) are cited in Kroll et al. (1997). See text for explanation of the data of Lueder (1995). The *vertical bar on a symbol* indicates $\pm 1\sigma$ uncertainty of $\ln k_{D^*}$ resulting from that in the structural data. For the *solid circles* (this work), the error *bars* are approximately the diameters of the symbols

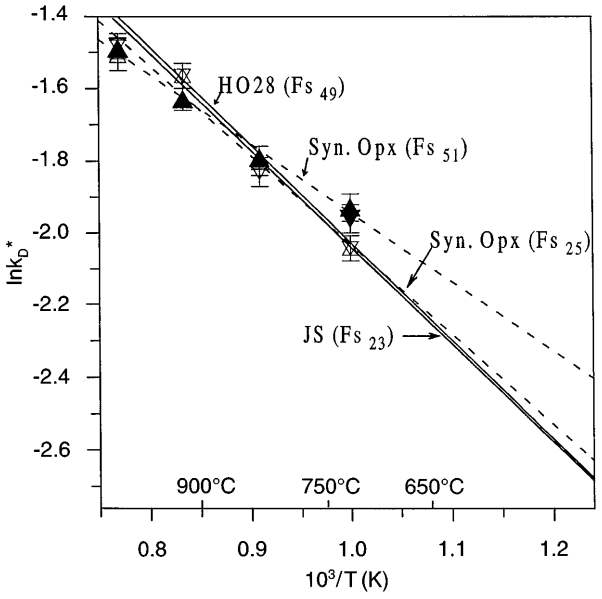

Fig. 3 Comparison of the $\ln k_{D^*}$ versus $1/T$ relations for natural orthopyroxenes with Fs_{23} and Fs_{49} determined in this study (*solid lines*) with those of synthetic binary orthopyroxenes (*dashed lines*) of similar composition (Fs_{25}: *open symbols*) and Fs_{51} (*solid symbols*) determined by Yang and Ghose (1994). Both sets of results are based on weighted structure refinements using RFINE90. See Fig. 1 for explanation of orientation of symbols

thickness (Skogby et al. 1992). We also decided not to include any other published site occupancy data which were determined by single crystal X-ray diffraction, as these either lacked sufficient procedural details to enable us to evaluate their quality or did not adequately demonstrate attainment of equilibrium site occupancy using high quality crystal-chemically constrained microprobe data for the bulk compositions of the crystals. An *a priori* selection of data based on experimental details is very important in the development of models from the data.

The data summarized in Fig. 2 show, reinforcing the conclusion of Ganguly and Domeneghetti (1996), that there is no significant compositional dependence of k_{D^*} in the range Fs_{19} and Fs_{75} when the compositions of orthopyroxene are close to the Fe-Mg binary. However, the data beyond this range cannot be reconciled with the much larger data set within it in terms of the thermodynamic models discussed above. The apparently anomalous behavior of the terminal segments may be due to either a change of the nature of the solution property in the terminal segments (Darken 1967) and/or an intrinsic problem of the single crystal X-ray technique in the determination of the site occupancies when the concentration of one of the components falls below a certain limit. We, thus, treated the available data in the range Fs_{19}–Fs_{75} separately from those in the terminal segments.

Stepwise statistical regression of the $\ln k_{D^*}$ versus X_{Fe^*} and T data according to the form of Eq. 1 in the compositional range Fs_{19}–Fs_{75} yields ($r^2 = 99.0\%$)

$$\ln k_{D^*} = -\frac{2557(\pm 49)}{T} + 0.547(\pm 0.048) \quad (3)$$

The $\ln k_D^*$ values were weighted by $1/[\sigma(\ln k_D^*)]^2$. As expected from the data illustrated in Fig. 2, the W parameters were rejected by the program (SPSS 8.0 for windows) as statistically insignificant. In Eq. 3 and elsewhere, the uncertainties represent 1σ values. Because we have only an approximate idea about the errors in the site occupancies arising from those in the compositional data, the variance of $\ln k_D^*$ used in the regression are those arising from the effects of the statistical errors of only the structural data. The inclusion of the JS sample in our data set may be questioned as this sample contained minute exsolution of clinopyroxene (Molin et al. 1991) which may interfere with some of the orthopyroxene reflections (Domeneghetti et al. 1996). (The clinopyroxene exsolutions were carefully avoided in the microprobe analysis of this sample.) Exclusion of the JS sample from our data set, however, did not lead to any significant change in the regressed expression of $\ln k_D^*$ (Eq. 3).

There are three orthopyroxene crystals in the compositional range $X_{Fe^*} = 0.11$–0.17 which have mutually similar but significantly lower k_D^* values than those of orthopyroxenes with $X_{Fe^*} = 0.19$–0.75 (Fig. 2). The data set at $X_{Fe^*} = 0.11$–0.17 can be adequately represented as ($r^2 = 95\%$)

$$\ln k_D^* = -\frac{2854(\pm 86)}{T} + 0.603(\pm 0.095) \quad (4)$$

We would like to emphasize that the site occupancies of the three orthopyroxene crystals at $X_{Fe^*} = 0.11$–0.17 were determined by two different groups following somewhat different procedures. Therefore, the difference between their k_D^* values from those of orthopyroxenes at $X_{Fe^*} = 0.19$–0.75 could be real. If not, then there are some inherent problems in the X-ray method at low Fe concentration which we are unable to identify. However, regardless of this potential problem, it should be possible to determine from Eq. 4 the T_C for cation ordering of an unknown sample with $0.11 < X_{Fe^*} < 0.17$, and comparable concentrations of the nonbinary components as in the three orthopyroxene crystals, if the site occupancies of the unknown samples are determined from single crystal X-ray data following the procedure outlined above.

There is only one sample at $X_{Fe} > 0.75$, and the data for this sample are incompatible with the rest of the data summarized in Fig. 2. Without more data at such high Fe concentration, it would not be appropriate to either include this apparently anomalous data within the main data set or invoke a different solution behavior in the high Fe terminal segment.

Precision of the thermometric calibrations

In order to test the internal consistency of our method and thermometric calibrations, we have annealed several natural orthopyroxene crystals with Fs_{51} at 750 and 850 °C, determined their site occupancies using RFINE90 following exactly the same procedure as discussed above, and calculated the equilibration temperatures from Eq. 3. The calculated temperatures were within 1 to −10 °C of the annealing temperatures. These comparisons provide some impression of the accuracy with which one may expect to retrieve the closure temperature of cation ordering of natural samples using the above calibrations, and following the procedure of site occupancy determination used in this work. Inclusion of these data within our primary data set did not have any effect on the result of the regression (Eq. 3).

Comparison with earlier calibrations

There have been several earlier calibrations of intracrystalline Fe-Mg fractionation in orthopyroxene as a function of composition and temperature, which are summarized and discussed by Kroll et al. (1997). With the exception of Yang and Ghose (1994) and Ganguly and Domeneghetti (1996), each calibration included all or most of the data available until then. Equations (3–4) should supersede the expressions derived by Yang and Ghose (1994) and Ganguly and Domeneghetti (1996) as the data sets used by them are included within the set used in this study.

Kroll et al. (1997) have also collected all available site partitioning data of orthopyroxene as a function of temperature and composition. However, they found the data to be highly inconsistent and thus subjected different subsets of the data to statistical regression within the framework of Eq. 2. Of these, they preferred the results of regression from one subset in the compositional range of Fs_{19}–Fs_{86} because of their better internal consistency. Test calculations show that the equation suggested by Kroll et al. (1997) yields T_C of natural samples with Fs between ~19 and 75 which are on the average ~15 °C higher than those calculated from Eq. 3. For Fs = 11–17, the T_C values determined from the expression of Kroll et al. (1997) are on the average ~75 °C lower than those determined from Eq. 4. This difference in T_C values would lead to a very large difference in the retrieved cooling rates (Ganguly et al. 1989; Kroll et al. 1997).

Excess configurational entropy of mixing and implication for solution model

Equations 3 and 4 permit calculation of the site occupancy data as a function of bulk composition and temperature from which one can directly calculate the configurational entropy of mixing. This calculation is independent of any mixing model except that involving the assumption that the cation distribution is random within each type of site. The excess configurational en-

tropy of mixing, ΔS^{XS}, was calculated as a function of bulk composition and T according to

$$\Delta S^{XS} = R \ln \Omega(\text{ord}) - R \ln \Omega(\text{ideal}) \quad (5)$$

where Ω(ord) and Ω(ideal) represent the number of geometric configurations in the ordered and completely disordered solid solution. For an ordered orthopyroxene crystal $(Fe_{X1}Mg_{(1-X1)})^{M1}(Fe_{X2}Mg_{(1-X2)})^{M2}Si_2O_6$ with a specific bulk composition, $X_{Fe} \equiv X$, Eq. 5 reduces to

$$\begin{aligned}\Delta S^{XS} = &-R[X1 \ln X1 + (1-X1)\ln(1-X1) \\ &+X2 \ln X2 + (1-X2)\ln(1-X2)] \\ &+ 2R[X \ln X + (1-X)\ln(1-X)] \end{aligned} \quad (6)$$

The calculated values of $-T(\Delta S^{XS})$, which constitute the ordering contribution to the excess Gibbs free energy of mixing, ΔG^{XS}, are illustrated in Fig. 4 as a function of X_{Fe} and T. As determined by RFINE 90, the site occupancies of the crystals with Fs $\leq$ 0.5 have standard deviations $\sim$0.001 (Tables 1–2), whereas those for crystals with Fs > 0.75 have standard deviations of $\sim$0.005 (Yang and Ghose 1994) (there are no measurements between Fs_{50} and Fs_{75}). The effects of these errors on the calculation of configurational entropies are shown in Fig. 4 for selected compositions within the two compositional ranges. The uncertainties in the bulk compositional data would expand this error by a factor of 2–3. Even accounting for these uncertainties, the configurational $T\Delta S^{XS}$ values calculated from the Fe-Mg ordering data are significantly different from those predicted from the model of Berman and Aranovich (1996), who suggested a simple mixture model for orthopyroxene with a $W^S = -2.68$ J/mol-K on two-cation basis. For comparison, the $-T\Delta S^{XS}$ values calculated from their model at 600 and 1000 °C are illustrated in Fig. 4 (this model also implies increase of ordering with increasing temperature if it is assumed that the vibrational spectrum of orthopyroxene is not significantly affected by the changes in the geometric configurations; see Ganguly and Saxena 1987 section 2.11).

The calculated ΔS^{XS} is symmetric to bulk composition at least for the compositional range Fs_{19} and Fs_{75} but it does not conform to the *parabolic* symmetry of a simple mixture at $T < 1000$ °C (Fig. 4). In order to fit the calculated ΔS^{XS} versus X_{Fe} relation, we used the general polynomial form suggested by Guggenheim (1937) to represent an excess mixing property (ΔY^{XS}) of a binary solution as a function of composition:

$$\Delta Y^{XS} = X_1 X_2 [A_0 + A_1(X_1 - X_2) + A_2(X_1 - X_2)^2 + \cdots] \quad (7)$$

When the A constants with odd subscripts become zero, the excess property becomes symmetric to composition.

The symmetric ΔS^{XS} versus X_{Fe} relation illustrated in Fig. 4 may be modeled very well by retaining only the A_0 and A_2 constants in the above polynomial. The fitted relations are shown by solid lines. The A_0 and A_2 terms are, however, functions of temperature (Fig. 5). We modeled their temperature dependencies according to the functional form of S(T) for the condition of linear dependence of C_p on T, but subject to the constraint that these parameters do not develop extremes in the range

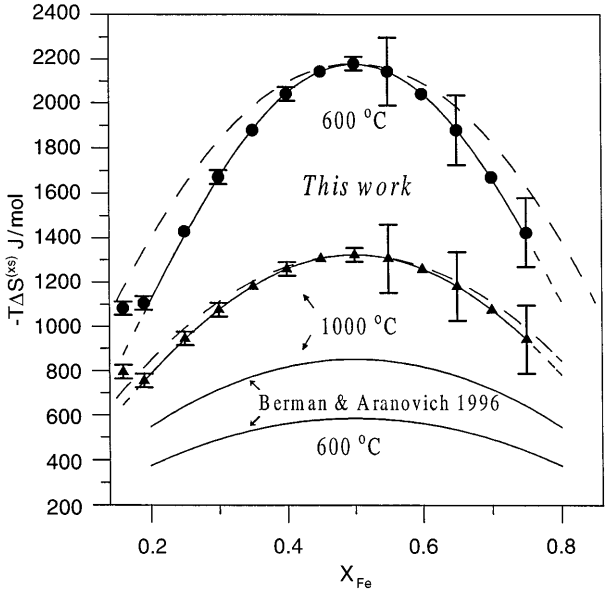

Fig. 4 Contribution of Fe-Mg ordering (2 cations per mole) in orthopyroxene ($-T\Delta S^{XS}$) to the excess Gibbs free energy of mixing as a function of T and X_{Fe}. The *thick solid lines* are fits to the calculated values (*solid symbols*), according to the 2-parameter symmetric solution model of Guggenheim (1937). The X_{Fe} range of the calculations corresponds to that of the experimental data used to develop the analytical expression of ΔS^{XS}. The *vertical bars* are maximum 1σ values of the calculated $T\Delta S^{XS}$ arising from the uncertainties of the structural data at the corresponding compositions. The *dashed lines* illustrate the parabolic symmetry of the "simple mixture" model. Also shown for comparison are the $-T\Delta S^{XS}$ values per 2-cation moles calculated according to the model of Berman and Aranovich (1996)

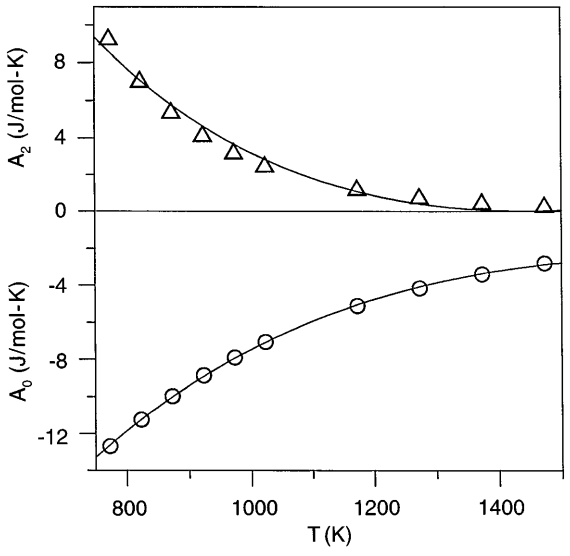

Fig. 5 Variation of the fitting parameters to ΔS^{XS} versus X_{Fe} data (Fig. 4) as a function of temperature. The *solid lines* represent fits to the calculated data (*triangles and circles*) according to Eq. (8). The data are for 2-cation moles

500–1200 °C. Thus, for the specified temperature range, we have

$$A_0^S = -268.67(\pm 6.57) + 41.31(\pm 1.10)\ln T - 0.0241(\pm 0.001)T \quad (8.1)$$

and

$$A_2^S = 338.14(\pm 31.69) - 53.90(\pm 5.25)\ln T + 0.0374(\pm 0.005)T \quad (8.2)$$

in units of J/mol-K (two-cation basis), where the superscript S implies an entropic parameter. The uncertainties are $\pm 1\sigma$ values resulting from the scatter of the A parameters (Fig. 5).

The above analysis suggests that orthopyroxene solid solution should be treated according to *two parameter symmetric model*, at least in the compositional range Fs_{19} to Fs_{75}, rather than as a simple mixture or a regular solution. Even beyond this compositional range, the deviation of the available data from the two-parameter symmetric model is quite small. The activity coefficients in this model are expressed by Redlich-Kister equations (e.g., Ganguly and Saxena 1987), but retaining only the A_0^G and the A_2^G terms.

Enthalpy of mixing

Von Seckendroff and O'Neill (1993) determined the Fe-Mg fractionation between olivine and orthopyroxene at 900–1150 °C, 16 kbar, and deduced a value of $W^G = 2145 \pm 614$ J/cation-mol ($\pm 1\sigma$) at 16 kbar from these data, assuming that both olivine and orthopyroxene behave as simple mixtures. Since there is no significant volume of mixing in the binary orthopyroxene solid solution (Chattilon-Colinet et al. 1983), the W^G (OPx) is almost independent of pressure. von Seckendroff and O'Neill (1993) also noted that their experimental data can be modeled almost equally well by constraining the olivine solution property to that ($W^G = 3700 \pm 800$ J/cation-mol) determined by Wiser and Wood (1991), which yielded a near ideal $W^G = 280 \pm 900$ J/cation-mol for orthopyroxene. A near ideality of $(Fe,Mg)SiO_3$ is also implied by the Fe-Mg exchange data of Lee and Ganguly (1988) between garnet and orthopyroxene, at least at $T \geq 1000$ °C, if one accepts that the Fe-Mg mixing in garnet is nearly ideal (Hackler and Wood 1989). Hayob et al. (1993) calculated the activity-composition relation of orthopyroxene from their experimental data on the quartz-ilmenite-rutile-orthopyroxene equilibrium. Their analysis suggests a small positive deviation from ideality for the binary orthopyroxene solid solution, but considering their uncertainties the retrieved activity data are compatible with an ideal mixing model.

Combining with the $T\Delta S^{XS}$ values calculated in this work (Fig. 4), the above W^G values for orthopyroxene yield $\Delta H^{XS}(Fs_{50}) = -828 \pm 225$ J/cation-mol, or -362 ± 153 J/cation-mol at 750 °C, depending on whether or not it is required to be compatible with the results of Wiser and Wood (1991) for olivine. More recent work (H. StC. O'Neill, personal communication) corroborated the W^G (olivine) determined by Wiser and Wood (1991) so that the first one should be the preferred value for $\Delta H^{XS}(Fs_{50})$. The *negative* excess enthalpy of mixing of orthopyroxene derived above is, however, in contrast to the *positive* excess enthalpy of mixing determined by Chattilon-Colinet et al. (1983) by heat of solution measurements of synthetic $(Fe,Mg)SiO_3$ in lead borate calorimeter. The W^H parameter fitted by von Seckendroff and O'Neill (1993) to the calorimetric data at 750 °C yields $\Delta H^{XS}(Fs_{50}) = 1187 \pm 625$ J/cation-mol. On the other hand, Berman and Aranovich (1996) suggested a value of $W^H = -2600$ J/cation-mol in their optimized data base for solution properties of minerals, which yields $\Delta H^{XS}(Fs_{50}) = -650$ J/cation-mol, in agreement with the values derived above.

The reason for the disagreement between the ΔH^{XS} derived from phase equilibria and Fe-Mg ordering data with that determined calorimetrically is not clear. However, as pointed out by Berman and Aranovich (1996), there are only three $(Fe,Mg)SiO_3$ compositions for which heat of solution were measured, and of these, two are compatible with the ideal mixing model within $\pm 1\sigma$ uncertainty width. An alternative explanation of this discrepancy is that the solid solutions have positive excess vibrational entropies which more than compensate their reduction of entropies due to ordering. Additional calorimetric measurements with improved accuracy will be very useful to clarify the problem.

Acknowledgements We are grateful to Dr. Robert Downs for his insightful advice on structure refinements and to Professor Herbert Kroll for valuable discussions, and for providing X-ray data for the orthopyroxene sample from an acapulcoite meteorite and the revised site occupancy data for a synthetic orthopyroxene sample. Thanks are due to Professor Linc Hollister for donation of the granulite sample used in this work, and to Dr. Ed Olsen for the donation of Steinbach meteorite sample from the collection of the Natural History Museum of Chicago. The paper has greatly benefited, in both substance and style, from the very careful reviews of Professors Herbert Kroll and Eric Essene. This research was supported by NASA grants NAGW 3638 and NAG 5-4716 to J.G. and by MURST and CNR-CSGA Padova grants to G.M.

References

Abrahams SC, Keve ET (1971) Normal probability plot analysis of error in measured and derived quantities and standard deviations. Acta Crystallogr A27: 157–165

Anovitz LM, Essene EJ, Dunham WR (1988) Order-disorder experiments on orthopyroxenes: implications for the orthopyroxene geospeedometer. Am Mineral 73: 1060–1073

Artioli G, Davoli G (1995) Low-Ca pyroxenes form LL-group chondritic meteorites: crystal structural studies and implications for their thermal histories. Earth Planet Sci Lett 128: 469–478

Berman RG, Aranovich LYa (1996) Optimized standard state and solution properties of minerals. I. Model calibration for olivine, orthopyroxene, cordierite, garnet, and ilmenite in the system FeO-MgO-CaO-Al_2O_3-TiO-SiO_2. Contrib Mineral Petrol 126: 1–24

Chatillon-Colinet C, Newton RC, Perkins D III, Kleppa OJ (1983) Thermochemistry of $(Fe^{2+}, Mg)SiO_3$ orthopyroxene. Geochim Cosmochim Acta 47: 1597–1603

Darken LS (1967) Thermodynamics of binary metallic solutions. Trans Metall Soc AIME 239: 80–89
Dollase WA, Newman WI (1984) Statistically most probable stoichiometric formulae. Am Mineral 69: 553–556
Domeneghetti MC, Molin GM, Tazzoli V (1985) Crystal-chemical implications of the Mg^{2+}-Fe^{2+} distribution in orthopyroxenes. Am Mineral 70: 987–995
Domeneghetti MC, Tazzoli V, Boffa Ballaran T, Molin GM (1996) Orthopyroxene from the Serra de Magé meteorite: a structure-refinement procedure for a *Pbca* phase coexisting with a *C2/c* exsolved phase. Am Mineral 81: 842–846
Finger LW, Prince E (1975) A system of FORTRAN IV computer programs for crystal structural computations. Nat Bur Stand Tech Note 854
Ganguly J (1982) Mg-Fe order-disorder in ferromagnesian silicates II.Thermodynamics, kinetics and geological applications. In: Saxena SK (ed) Advances in physical geochemistry, 2. Springer Verlag, Berlin Heidelberg New York Tokyo, pp 58–99
Ganguly J (1986) Disordering energy versus disorder in minerals: a phenomenological relation and application to orthopyroxene. J Phys Chem Solids 47: 417–420
Ganguly J, Domeneghetti MC (1996) Cation ordering of orthopyroxenes from the Skaergaard intrusion: implications for the subsolidus cooling rates and permeabilities. Contrib Mineral Petrol 122: 359–367
Ganguly J, Saxena SK (1987) Mixtures and mineral reactions. Springer-Verlag, Berlin Heidelberg New York Tokyo
Ganguly J, Bose J, Ghose K (1989) Fe^{2+}-Mg ordering in orthopyroxenes and the cooling rates of meteorites. Lunar Planet Sci XX: 331–332
Ganguly J, Yang H, Ghose S (1994) Thermal history of mesosiderites: quantitative constraints from compositional zoning and Fe-Mg ordering in orthopyroxenes. Geochim Cosmochim Acta 58: 2711–2723
Ganguly J, Stimpfl M, Molin G (1997) Orthopyroxene chronometry of meteorites. II. Towards a general relation between cooling rate and closure temperature of cation ordering and application to the Steinbach meteorite. Lunar Planet Sci XXXVIII: 391–392
Ghose S (1965) Mg^{2+}-Fe^{2+} order in an orthopyroxene, $Mg_{0.93}Fe_{1.07}Si_2O_6$. Zeit Kristallogr 122: 81–99
Guggenheim EA (1937) Theoretical basis of Raoult's law. Trans Faraday Soc 33: 151–159
Haack H, Scott ERD, Love SG, Brearley AJ, McCoy TJ (1996) Thermal histories of IVA stony-iron meteorites: evidence for asteroid fragmentation and reaccretion. Geochim et Cosmochim Acta 60: 3103–3113
Hackler RT, Wood BJ (1989) Experimental determination of Fe and Mg exchange between garnet and olivine and estimation of Fe-Mg mixture properties in garnet. Am Mineral 74: 994–999
Hawthorone FC, Ito J (1978) Refinement of the crystal structures of $(Mg_{0.776}Co_{0.224})SiO_3$ and $(Mg_{0.925}Mn_{0.075})SiO_3$. Acta Crystallogr B34: 891–893
Hayob JL, Bohlen SR, Essene EJ (1993) Experimental investigation and application of the equilibrium rutile + orthopyroxene = quartz + ilmenite. Contrib Mineral Petrol 115: 18–35
Hollister LS (1982) Metamorphic evidence for rapid (2 mm/year) uplift of a portion of the Central Gneiss Complex, Coast Mountains B. C. Can Mineral 20: 319–332
International Tables For X-Ray Crystallography, 4 (1974) Kynoch Press, Birmingham pp 99–101, 293–294
James F, Roos M (1975) MINUIT, a system for function minimization and analysis of the parameter error and correlations. Comput Phys Commun 10: 343–347, CERN/DD, Int Rep 75/20
Kirfel A (1996) Cation distributions in olivines and orthopyroxenes: an interlaboratory study. Phys Chem Miner 23: 503–519
Kroll H, Lueder T, Schlenz H, Kirfel A, Vad T (1997) The Fe^{2+}-Mg distribution in orthopyroxene: a critical assessment of its potential as a geospeedometer. Eur J Mineral 9: 733–750
Lee HY, Ganguly J (1988) Equilibrium compositions of coexisting garnet and orthopyroxene: experimental determinations in the system FeO-MgO-Al_2O_3-SiO_2, and applications. J Petrol 29: 93–113
Lueder T (1995) Fe^{2+},Mg-Verteilunge und Abkühlraten von Fe-armen natürlichen Orthopyroxenen. PhD diss Westfälishe Wilhelms-Univ, Münster
Molin GM, Saxena SK, Brizi E (1991) Iron-magnesium order-disorder in an orthopyroxene crystal from the Johnstown meteorite. Earth Planet Sci Lett 105: 260–265
Molin GM, Tribaudino M, Brizi E (1994a) Zaoyang chondrite cooling history from Fe^{2+}-Mg intracrystalline ordering in pyroxenes. Mineral Mag 58: 143–150
Molin G, Domeneghetti MC, Salviulo G, Stimpfl M, Tribaudino M (1994b) Antarctic FRO90011 lodranite: cooling history from pyroxene crystal chemistry and microstructure. Earth Planet Sci Lett 128: 479–487
North ACT, Phillips DC, Mathews FS (1968) A semi empirical method of absorption correction. Acta Crystallogr A24:351–359
Sack RO (1980) Some constraints on the thermodynamic mixing properties of Fe-Mg orthopyroxenes and olivines. Contrib Mineral Petrol 71: 257–269
Saxena SK, Ghose S (1971) Mg^{2+}-Fe^{2+} order-disorder and the thermodynamics of the orthopyroxene crystalline solution. Am Mineral 56: 532–559
Schlenz H (1995) Orthopyroxene als potentielle Geospeedometer. PhD Diss Westfälishe Wilhelms-Univ, Münster
Sheldrick GM (1993) SHELXL93. Program for crystal structure refinement. Univ Göttingen, Germany
Skogby H (1992) Order-disorder kinetics in orthopyroxenes of ophiolite origin. Contrib Mineral Petrol 109: 471–478
Skogby H, Annersten H, Domeneghetti MC, Molin GM, Tazzoli V (1992) Iron distribution in orthopyroxene: a comparison of Mössbauer spectroscopy and X-ray refinement results. Eur J Mineral 4: 441–452
Thompson JB Jr (1969) Chemical reactions in crystals. Am Mineral 54: 41–375
Thompson JB Jr (1970) Chemical reactions in crystals: corrections and clarification. Am Mineral 55: 528–532
Tokonami M (1965) Atomic scattering factor for O^{2-}. Acta Crystallogr 19: 486
von Seckendorff V, O'Neill H StC (1993) An experimental study of Fe-Mg partitioning between olivine and orthopyroxene at 1173, 1273 and 1423 K and 1.6 GPa. Contrib Mineral Petrol 113: 196–207
Wiser NM, Wood BJ (1991) Experimental determination of activities in Fe-Mg olivine at 1400 K. Contrib Mineral Petrol 108: 146–153
Yang H, Ghose S (1994) In-situ order-disorder studies and thermodynamic properties of orthopyroxene $(Mg,Fe)_2Si_2O_6$. Am Mineral 79: 633–643
Zema M, Domeneghetti MC, Molin G, Tazzoli V (1997) Cooling rates of diogenites: a study of Fe^{2+}-Mg ordering in orthopyroxene by X-ray single-crystal diffraction. Meteoritics Planet Sci 32: 855–862